

Water film motor driven by alternating electric fields: Its dynamical characteristics

Zhong-Qiang Liu,¹ Guang-Cai Zhang,² Ying-Jun Li,^{1,*} and Su-Rong Jiang³

¹State Key Laboratory for GeoMechanics and Deep Underground Engineering, SMCE,
China University of Mining and Technology, Beijing 100083, China

²National Key Laboratory of Computational Physics, Institute of Applied Physics and Computational Mathematics, Beijing 100088, China

³Qindao College, Qingdao Technological University, Qingdao 266106, China

(Received 3 January 2012; published 26 March 2012)

The “liquid film motor,” a novel device with important implications for basic research and technology, is analyzed. It works perfectly with both direct current (dc) and alternating current (ac) fields. We develop a mathematical model describing electrohydrodynamical (EHD) motions induced by ac fields, which are more complex and have wider technological applications than those produced by dc fields. The main characteristics of these motions, derived in our paper and in full agreement with the experimental ones, are as follows: (i) **Rotation of the film requires that the frequencies of the ac fields are exactly the same and their magnitudes surpass a threshold, which depends on their phase difference.** (ii) **Vibrations may be induced by fields with different frequencies.** (iii) **The EHD motions strongly depend on the polarization induced by the external electric field.** However, **these motions are little affected by the liquid’s electrical conductivity, viscosity, dielectric constant, and density.** Our model also predicts several features, which have yet to be experimentally verified.

DOI: 10.1103/PhysRevE.85.036314

PACS number(s): 47.65.-d, 68.15.+e, 83.60.La, 77.22.Ej

I. INTRODUCTION

Currently, the study of the impact of electric fields on liquid films is an endeavor of major theoretical and technological importance for advancements in physics, biophysics, and engineering [1,2]. During the last decades, numerous phenomena, with major potential applications in industry, have been observed when fields are applied to liquid films. For example, electrically driven motions are used in microfluidic systems to mix or phase separate liquids or particles [3,4]. In this context, the electrohydrodynamical (EHD) motions of suspended liquid films have attracted considerable attention. These motions were observed in freely suspended liquid crystal films [5–8] and in suspended polar liquid films, e.g., films of water or its solutions [9–12].

Very recently, these motions have been harnessed to produce the “liquid film motor” [10–12]. This motor consists of a quasi-two-dimensional electrolysis cell in an external in-plane electric field, \mathbf{E}_{ext} . An electrolysis current $\mathbf{J}_{\text{el}} = \gamma \mathbf{E}_{\text{el}}$ (γ is electric conductivity and \mathbf{E}_{el} is the electrolysis electric field) crosses \mathbf{E}_{ext} . By setting the right conditions, the film will rotate. **The onset of rotation depends on the polarity of the liquid’s molecules, the thickness of the film, and the magnitudes, directions, and frequencies of the fields.** Rotation was observed only for polar liquids such as water, its solutions, aniline, anisole, chlorobenzene, and diethyl oxalate. The direction and speed of the rotation are controlled by manipulating the direction and strength of the applied electric fields. These qualities led to the device’s name, “liquid film motor.” Alternating current (ac) as well as direct current (dc) fields can induce rotation of the film. Experiments have shown that the dynamics induced by ac fields is more complex than that induced by dc fields. (In the rest of this paper, we will refer to a rotating liquid film driven by dc or ac fields, respectively, as dc motor and ac motor.) The main experimentally observed characteristics of these motors are [10–12] as follows.

dc motor:

(a) For nonvanishing \mathbf{E}_{ext} and \mathbf{J}_{el} , whenever \mathbf{E}_{ext} or the electrolysis voltage U_{el} exceeds a threshold, the film rotates. The threshold fields obey a simple scaling relation.

(b) The direction of rotation within the EHD-induced vortices obeys a simple right-hand rule, $\mathbf{E}_{\text{ext}} \times \mathbf{J}_{\text{el}}$.

(c) Angular velocity measurements show that points closer to the center of the vortices rotate faster than those farther away, i.e., the angular velocity is a decreasing function of the points’ distance from the center of the vortices.

ac motor:

The fields’ frequencies, magnitudes, and the difference in their phases strongly influence the dynamics of the liquid film in the following ways.

(a) Whenever the frequencies of \mathbf{E}_{ext} and U_{el} are exactly the same, the film may rotate. The phase difference of the fields and their magnitudes affect the threshold for rotation and the angular velocities. The dynamical characteristics of the rotation, measured for frequencies in the range of 50 Hz up to 40 kHz, are the same as those of the dc case.

(b) Fields with different frequencies induce vibrations with beating frequencies. Such fields do not lead to any rotation.

The inventors of the water film motor presented several arguments against the possibility of generation of the observed EHD flows by the **edge effects** [11]. These arguments were based on a series of experimental findings. Instead of the edge effects, the experimentalists attributed the specific characteristics of the observed flows to the **intrinsic polarity** of the water molecules [11,12]. Indeed, they did observe that \mathbf{E}_{ext} and \mathbf{J}_{el} induce very similar flows in other polar liquids, e.g., aniline, anisole, chlorobenzene, and diethyleoxalate. In films of weakly polar or nonpolar liquids, no clearly distinguishable rotational movement was observed. For example, in the stable 1-dodecene liquid films, experimentalists did not succeed in inducing any rotation.

Notwithstanding the experimentally deduced insights, theoreticians did attempt to derive a rotational flow in a film

*lyj@aphy.iphy.ac.cn

generated by the edge effects [13]. They proposed a model which provides a possible explanation for the rotation of the dc motor. However, in contradiction to experimentally observed characteristic (c), according to the model, the rotation starts at the edges. They did not model the ac motor. In another attempt to explain the phenomena of the liquid film motor, theoreticians focused on the action of the mechanical moments on the liquid [14]. This enabled them to study the stationary rotation characteristics of the dc motor and to explain its characteristics (b) and (c). However, its characteristic (a) remained unexplained, as did the phenomena pertaining to the ac motor.

Challenged to develop a model capable of accounting for all of the observed phenomena, in a previous study, we presented a model in which the electric dipole moments of the liquid molecules play a significant role in the generation of the rotational flows [15]. Our model successfully explained the observed characteristics (a)–(c) of the dc motor. To the best of our knowledge, no explanation currently exists for the more complex dynamical processes in the ac motor. A thorough understanding of these processes is important. The potential technological applications of the ac motor are wider than those of the dc motor.

The goal of our paper is to present a model for the ac motor. In particular, we aim at the following: (a) derivation of the dynamical equations describing the motions in the motor's film, (b) derivation of the equations for the threshold values of the E_{ext} and E_{el} fields required for starting the film's vibrations and rotations, (c) analysis of the effects of the frequencies and phases of the applied E_{ext} and E_{el} fields on the dynamics of the film, and (d) predicting yet unreported characteristics of the motor, which might prove to be technologically advantageous.

The outline of this paper is as follows: In Sec. II, we present a model for the ac motor and derive the general equations describing its EHD motions. We will focus on motors composed of water films. Currently, the available experimental data mainly pertain to such films. We will show that our model also applies to other polar liquids. In Sec. III, we derive a series of specific characteristics of this motor, e.g., the threshold conditions for the onset of vibration and rotation of the film, the influence of the frequencies of the ac fields, and their phase differences on EHD motions. We compare these characteristics with the experimental ones reported in the literature. The comparison enables evaluation of our model and provides an explanation for the experimentally observed characteristics of the ac motor. In Sec. IV, we present a concise summary of our numerous results. Our conclusions we present in Sec. V. We stress that in this paper we only theoretically derive characteristics of the ac motor. We do not report any new experimental data. All of the experimental results cited in our paper were obtained by different research groups and reported in the literature.

II. MODEL OF WATER FILMS AND THEIR DYNAMICS

A. The suspended water film

We assume that the very thin films wherein the experimentalists succeeded to induce rotational flows, i.e., water or other polar liquid films placed in sufficiently strong E_{ext} , can

be adequately represented by a Bingham plastic fluid. For the dc motor, this assumption indeed enabled us to successfully explain the observed phenomena [15]. In our previous paper, we detailed the model and presented the experimental and theoretical evidence corroborating it [15]. Since the model is rather innovative and lately additional supporting experimental evidence has accumulated, we concisely summarize these.

The plasticity of the film results from long-ordered chains composed of coherent domains with an electric dipole moment [15–17]. These chains are analogous to the particle chains responsible for the plastic behavior of electrorheological fluids [18]. The coherent domains' diameter typically reaches hundreds of micrometers (μm) [16,17,19,20]. Their dipole moments result from the alignment of the electric dipole moments of their coherently oscillating molecules [16,17,19,20].

The formation of coherence domains (CDs) in water at room temperatures and pressures, as well as in other liquids composed of polar molecules with a sufficiently large electric dipole moment, was recognized in 1988 [19]. Within the context of quantum field theory (QFT), it was shown that long-range interactions (μm range interactions mediated through the electromagnetic field) cause some types of polar liquid molecules, in particular, water (H_2O) molecules, to distribute over two phases: (1) a low-density coherent phase, composed of domains wherein the molecules coherently oscillate, resonating in-phase with a coherently condensed electromagnetic field; and (2) a high-density noncoherent phase, composed of randomly moving molecules which are trapped in the interstices among the CDs. During the last two decades, a series of theoretical and experimental studies, undertaken by several independent research groups, have investigated the properties of the two phases and identified their role in various phenomena [19–23]. Within this context, we particularly emphasize (i) the recent extensive small-angle x-ray scattering experiments providing evidence for two phases of water having different densities and orderings [24], and (ii) the identified correspondence between the domain characteristics as predicted by QFT and the experimentally observed ones [23].

Various CD types have been identified. Concerning the above-mentioned CD type with an electric dipole moment, QFT indicates that in bulk liquid these domains are oriented randomly [19,20]. At interfaces, however, these domains are stabilized by the boundaries [16,17,19,20]. Consequently, in the presence of substrates or few solute particles, a net polarization exists [25].

Very recent findings conform to the QFT results: (i) Long-distance correlation in the longitudinal part of dipole-dipole correlations was identified in liquid water [26]. (ii) An anomalously slow relaxation process, attributed to long-range interactions, has been observed in water. The process is about four orders of magnitude slower than the viscosity-related structural main relaxation. The process has also been observed in alcohols [27]. A similar relaxation process was measured in polymers and glass-forming liquids [28]. Just as for the polymers and glass-forming liquids, the observed solid behavior of submillimeter-sized samples in water and alcohol has also been ascribed to this relaxation process. (iii) Measured orientation relaxation times for interfacial water molecules at neutral and ionic interfaces are significantly slower than that

of bulk water [29]. (iv) NMR spectroscopy showed that for water adjacent to hydrophilic surfaces, spin-lattice relaxation times and self-diffusion coefficients are smaller, i.e., **dynamics is slower**, than for bulk water [30].

External electric fields induce the CDs with their electric dipole moment to organize in superdomains [16,19,21,31]. According to QFT, for polar liquids, the application of an electric field causes the formation of long-ordered chains of **low-entropy aligned coherent dipolar domains** [16,31]. The electric-field-induced chain formation of dipolar spheres has also been identified by other approaches, e.g., integral equation theory in the reference hypernetted chain approximation, Monte Carlo simulations, and molecular dynamics simulations [32]. Two-dimensional (2D) neutron scattering has evidenced formation of such chainlike long-range molecular ordering within a D₂O bridge [33].

On locating a film composed of water or another polar liquid (containing CDs with an electric dipole moment) in an E_{ext} of a parallel-plate capacitor, it will **reach polarization equilibrium** [15,32]. In very thin films, e.g., hundreds of nanometers or less, **the equivalent dipole moment per unit volume is considerably larger**. The dipole moment of each domain is almost **completely parallel to E_{ext}** . The disruptive role of **thermal collisions gets neutralized by E_{ext} and the surface tension**. Moreover, **the restricted motion of the superdomains in the quasi-two-dimensional space is also advantageous for the alignment of the dipoles**. However, for relatively thick films (or bulk liquid), the motions of the superdomains are less restricted and, in the absence of surface tension, thermal aggression hinders the alignment of all dipole moments with E_{ext} . One can imagine that the directions of all dipole moments of CDs are relatively random in a space within a conical surface, whose axis is a straight line parallel to E_{ext} . Consequently, **the equivalent dipole moment per unit volume is a decreasing function of the thickness of the film**.

For a polar liquid film located in an E_{ext} , the application of an electrolysis electric field E_{el} causing an electric current induces a torque [15]. A sufficiently large E_{el} , crossing E_{ext} , **will impede on the polarization equilibrium**. However, E_{el} only exists within the liquid film. In contrast, E_{ext} , which plays a dominant role in the polarization, spans the whole space between two plates of a large parallel-plate capacitor. The strongly correlated motions of the CDs' coherently oscillating molecules imply that **it is impossible to touch one molecule without affecting all of the others** [17,21]. Therefore, **E_{ext} will rapidly reestablish the polarization equilibrium**. The continuous destructive effect of E_{el} on the polarization equilibrium maintained by E_{ext} **creates a torque perpendicular to the liquid thin film**. In other words, the continuous competition between the destruction and the reestablishment of the polarization equilibrium may induce EHD motions in the liquid film.

The onset of rotation requires that **the torque exerted on superdomains and their CDs is larger than the maximum static resistance torque arising from the yield stress**. With the magnitude of the torque depending on the dipole-moment directions of their CDs as well as the equivalent dipole moment per unit volume, which as noted above is a decreasing function of the thickness of the film, **the onset of rotational motion depends on the thickness of the film**. Indeed, experiments have

shown that production of both dc and ac water motors requires films with a thickness of less than 1 μm [11].

In regard to the above, from the macroscopic viewpoint, a compartment of a very thin polar liquid film located in an E_{ext} may be modeled as an equivalent electric dipole. The application of an E_{el} to such a film may cause shearing flows. Accordingly, such a liquid film corresponds to a Bingham plastic fluid with an equivalent electric dipole moment.

For a Bingham plastic fluid, for a simple shearing flow $u = u(y)$, the constitutive relation is [34]

$$\frac{\partial u}{\partial y} = \begin{cases} 0 & (\tau < \tau_0) \\ (\tau - \tau_0) / \mu & (\tau \geq \tau_0), \end{cases} \quad (1)$$

where τ denotes the **shear stress**, τ_0 is the so-called **yield stress**, μ represents the **plastic viscosity**, and y is the direction perpendicular to the flow velocity. Equation (1) indicates that flows occur in the liquid film, i.e., the film behaves like a fluid, when the shear stress is larger than the yield stress τ_0 .

We model the water film as a flat (two-dimensional) liquid, i.e., we assume its height h equals 0. This assumption corresponds with the above-mentioned findings that only very thin films can conspicuously rotate in the presence of E_{ext} and E_{el} [11].

Inspired by the experimentally observed stable disklike ring structure of the rotating liquid films, i.e., two-dimensional disks with radius r and width dr , we model the film as a series of **concentric circular disks** in a polar coordinate system (r, θ) . Movies of the experimentally observed EHD motions show that in circle-shaped liquid films, E_{ext} and E_{el} fields induce concentric circular flows [35]. In rectangular films with an aspect ratio close to 1, **concentric circular flows** cover most of the liquid. However, close to the edges, **rectangular-shaped streams** with smoothed smeared-out corners appear. These streams hint that **near the edges, in particular near the corners, stabilization of the electric dipoles of the CD and the resulting viscosity of the liquid is larger than in the remainder of the film**. Such **boundary effects** are indeed predicted by QFT [17]. An in-depth study of the **perturbation of the circular flows by edges and the resulting zonal structures** is important for extracting valuable information on the film's **molecular organization and intermolecular interactions**. Such a study will enable the refinement of the concentric circular disk model. However, the required analysis is beyond the scope of this paper's attempt to model the ac motor. Accordingly, we **neglect the edge-induced small perturbations of the flows** in this model, i.e., **we assume μ is a constant**.

As to other potential refinements of our liquid film model, we note that **the inclusion of mass transfer between the circular disks may be desirable**. A future study, examining such mass transfer, could illuminate the fluid nature of the film. As to **gravitational effects**, we assume that these are much smaller than the surface forces of the film and accordingly can be ignored.

B. Dynamics of the water film

The torque was derived in our previous paper [15]. There the torque exerted on a disk with radius r and width dr was deduced from the partial derivative of M_{rd} with respect to r . For M_{rd} holds $M_{\text{rd}} = M_{\text{curd}} + M_{\text{Bd}}$, where M_{rd} , M_{curd} , and

\mathbf{M}_{Bd} , respectively, denote the resultant torque, the accelerating torque, and the drag torque exerted on a disk with radius r . The term \mathbf{M}_{curd} results from the interaction between the equivalent dipole moment \mathbf{P} and the electrolysis electric field \mathbf{E}_{el} . \mathbf{M}_{Bd} derives from the yield stress and the viscous force in a Bingham plastic fluid. The direction of the accelerating torque, in correspondence with the vortices observed in the laboratory, obeys a right-hand rule, $\mathbf{P} \times \mathbf{E}_{\text{el}}$ (or $\mathbf{E}_{\text{ext}} \times \mathbf{E}_{\text{el}}$). The contribution of the hydrodynamics pressure p to the resultant torque vanishes because p is a periodic function of the angle θ , i.e., $p(\theta) = p(\theta + 2\pi)$.

By applying the rotational form of Newton's second law to the single disks of the water film, in Ref. [15], we derived their dynamical equation in crossed \mathbf{E}_{ext} and \mathbf{E}_{el} , i.e.,

$$u_t = \frac{\mu}{\rho r^2} (r^2 u_{rr} + r u_r - u) + \frac{\Delta(t)}{\rho r} \quad (0 \leq r \leq R, t > 0). \quad (2)$$

Here, u_t denotes the first partial derivative of the linear velocity $u(r, t)$ of the disk's rotation with respect to time t ; u_r and u_{rr} , respectively, represent the first and the second partial derivative of $u(r, t)$ with respect to radius r ; μ and ρ , respectively, are the plastic viscosity and the density of the fluid; $\Delta(t)$ is the driving source of the motions of the liquid film at time t , i.e., it represents the resultant moment exerted on the liquid film; $R = l/2$ is half of the side-length l of the square film (or the radius of the circle-shaped film).

To expound the functional form of $\Delta(t)$, derived in Ref. [15], we let M_{am} and M_f , respectively, symbolize the maximum of the accelerating torque and the maximum static drag torque exerted on a superdomain CD chain in the film. When $M_{\text{am}} < M_f$, i.e., $\Delta(t) \equiv 0$, the film remains static. When $M_{\text{am}} > M_f$, $\Delta(t) \neq 0$ and EHD motions appear in the film. The instantaneous value of $\Delta(t)$ is $|B(t)| - 2\tau_0$. Here, $|B(t)|$ denotes the absolute value of $B(t)$. As can be learned from Sec. IV in Ref. [15], $B(t)$ was derived from \mathbf{M}_{curd} and $-2\tau_0$ was derived from \mathbf{M}_{Bd} , that is, $B(t)$ and $-2\tau_0$, respectively, represent the accelerating torque and the drag torque exerted on the liquid film. For $B(t)$ holds $B(t) = \varepsilon_0(1 - 1/\varepsilon_r)E_{\text{ext}}(t)E_{\text{el}}(t)\sin\theta_{\text{EJ}}$ [15], where ε_0 and ε_r , respectively, are the dielectric constant of the vacuum and the relative dielectric constant of the liquid; $E_{\text{ext}}(t)$ and $E_{\text{el}}(t)$, respectively, denote the magnitudes of the external electric field \mathbf{E}_{ext} and of the electrolysis electric field \mathbf{E}_{el} at time t . θ_{EJ} is the angle between \mathbf{E}_{ext} and \mathbf{E}_{el} (or \mathbf{J}_{el}). Since the resultant torque is perpendicular to the liquid film, pointing "up" or "down," $\Delta(t)$ may be described by $(|B(t)| - 2\tau_0)$ or $-(|B(t)| - 2\tau_0)$. Thus, $\Delta(t)$ reads

$$\Delta(t) = \begin{cases} 0 & (|B(t)| < 2\tau_0) \\ B(t) - 2\tau_0 & (B(t) \geq 2\tau_0) \\ B(t) + 2\tau_0 & (B(t) \leq -2\tau_0) \end{cases} \quad (3)$$

There are two boundary conditions and an initial condition for Eq. (2): the disappearance of the linear velocity at $r = 0$ and $r = R$, and the liquid film is static at $t = 0$, i.e.,

$$u(r, t)|_{r=0} = 0, \quad u(r, t)|_{r=R} = 0, \quad (4)$$

and

$$u(r, t)|_{t=0} = 0. \quad (5)$$

Equation (2) is a typical diffusion equation with source. The general solution to it can be deduced by the Green function technique [36]. It reads

$$u(r, t) = \int_0^t d\varsigma \int_0^R G(r, t; \xi, \varsigma) f(\xi, \varsigma) d\xi, \quad (6)$$

where

$$G(r, t; \xi, \varsigma) = \sum_{n=1}^{\infty} \frac{2\xi}{R^2 J_0^2(\kappa_n)} J_1\left(\frac{\kappa_n r}{R}\right) J_1\left(\frac{\kappa_n \xi}{R}\right) e^{-\frac{\mu}{\rho} \frac{\kappa_n^2}{R^2} (t-\varsigma)}, \quad (7)$$

$$f(\xi, \varsigma) = \frac{\Delta(\varsigma)}{\rho \xi}. \quad (8)$$

Here, κ_n denotes the n th zero point of the $J_1(Z)$ ordinary Bessel function of order one, and $J_0(Z)$ is the ordinary Bessel function of order zero. Equation (7) indicates that motions of the liquid film consist of many spatial modes expressed by the Bessel functions of order one, $J_1(\kappa_n r/R)$. Equation (8) shows that $\Delta(t)$ determines the dynamics of the liquid film in the crossed electric fields.

The functional form of $\Delta(t)$ differs for ac and dc applied fields. In Ref. [15], we theoretically derived the functional form of $\Delta(t)$ for dc applied fields. To elucidate the difference between the dynamics of the ac and dc motor, in Sec. II B1, we first concisely summarize the characteristics of the dc motor. In Sec. II B2, we will derive the functional form of $\Delta(t)$ for ac applied fields.

1. Dynamics induced by applied dc fields

In the dc case, $\Delta(t)$ as given by Eq. (3) is independent of time t , enabling one to obtain the linear velocity of the rotation of the liquid film from Eqs. (6)–(8) [15]:

$$u_{\text{DC}}(r, t) = \Delta(t) \sum_{n=1}^{\infty} C_n J_1\left(\frac{\kappa_n r}{R}\right) (1 - e^{-a_n t}), \quad (9)$$

where

$$C_n = \frac{2R}{\mu} \frac{1 - J_0(\kappa_n)}{\kappa_n^3 J_0^2(\kappa_n)}, \quad a_n = \frac{\mu}{\rho} \frac{\kappa_n^2}{R^2}. \quad (10)$$

Equations (3) and (9) elucidate the EHD motions of the liquid film motor induced by the torques exerted on it, i.e., state of rest, and anticlockwise and clockwise rotation. Whenever the driving torque can continuously break the plastic structure of the liquid film, the film rotates. Otherwise, it remains static. Thus by equalizing the second or third line in Eq. (3) to zero, we directly obtain the scaling relation of the threshold fields [15], i.e.,

$$E_{\text{ext}} U_{\text{el}} \sin \theta_{\text{EJ}} = \pm \frac{2\tau_0 l}{\varepsilon_0 (1 - 1/\varepsilon_r)}. \quad (11)$$

Here, $U_{\text{el}} = E_{\text{el}} l$ is used, where U_{el} and l , respectively, denote the electrolysis voltage and the side-length of the electrolysis cell. In our previous paper, we showed that Eq. (11) is in good agreement with the experimental data [15].

2. Dynamics induced by applied ac fields

The experimentally observed dynamics induced by ac fields is more complex than that generated by dc fields. In addition to the state of rest or rotational motion, ac fields can cause the film to vibrate [11]. From a theoretical viewpoint, the state of rest implies $u(r,t) \equiv 0$, the vibration implies $u(r,t) \neq 0$ and $\overline{u(r,t)} = 0$, and the rotation implies $\overline{u(r,t)} \neq 0$, where $\overline{u(r,t)}$ is the time average of the linear velocity, i.e.,

$$\overline{u(r,t)} = \frac{1}{T} \int_0^T u(r,t) dt, \quad (12)$$

wherein the overbar represents the time average over one period T of the driving source. The foregoing together with Eqs. (12), (6), and (8) indicate that to derive the conditions for rotation versus vibration of the liquid film, we have to derive the functional form of the dependence of $u(r,t)$ on $\Delta(t)$. Since $\Delta(t)$ is a periodic function, on defining its period as $T = 2\pi/\omega$, its Fourier series expansion is

$$\Delta(t) = \sum_{m=0}^{\infty} (D_m \cos \omega_m t + H_m \sin \omega_m t), \quad (13)$$

where $\omega_m = m\omega$, $m = 0, 1, 2, \dots$, and coefficients D_m and H_m are determined by

$$\begin{aligned} D_0 &= \frac{1}{T} \int_0^T \Delta(t) dt = \overline{\Delta}, & D_m &= \frac{2}{T} \int_0^T \Delta(t) \cos \omega_m t dt, \\ H_m &= \frac{2}{T} \int_0^T \Delta(t) \sin \omega_m t dt & (T = 2\pi/\omega, m = 1, 2, \dots). \end{aligned} \quad (14)$$

Using Eqs. (6)–(8), (13), and (14), we have

$$\begin{aligned} u(r,t) &= \sum_{m=0}^{\infty} \sum_{n=1}^{\infty} C_n D_m J_1 \left(\frac{\kappa_n r}{R} \right) \frac{\cos \gamma_{m,n}}{\cos \varphi_m} \\ &\times [\cos(\omega_m t - \gamma_{m,n} - \varphi_m) - e^{-a_n t} \cos(\gamma_{m,n} + \varphi_m)], \end{aligned} \quad (15)$$

where

$$\gamma_{m,n} = \arctan(\omega_m/a_n), \quad \varphi_m = \arctan(H_m/D_m), \quad (16)$$

and C_n and a_n are determined by Eq. (10). Since the transient-state process vanishes when time is long enough, we only consider $u(r,t)$ without the transient-state terms, i.e., Eq. (15) becomes

$$\begin{aligned} u(r,t) &= \frac{\overline{\Delta}}{2\mu} r \ln \frac{R}{r} + \sum_{m=1}^{\infty} \sum_{n=1}^{\infty} C_n D_m J_1 \left(\frac{\kappa_n r}{R} \right) \\ &\times \frac{\cos \gamma_{m,n}}{\cos \varphi_m} \cos(\omega_m t - \gamma_{m,n} - \varphi_m), \end{aligned} \quad (17)$$

wherein Eq. (14) has been invoked. From Eq. (17), we obtain the average linear velocity, i.e.,

$$\overline{u(r,t)} = \frac{\overline{\Delta}}{2\mu} r \ln \frac{R}{r}. \quad (18)$$

The above analysis shows that the EHD motions of the liquid film induced by the crossed electric ac fields depend on the properties of the driving source and that it is feasible to deduce criteria for the different motion types by analyzing $\Delta(t)$. For

$\Delta(t) \equiv 0$, the film is in the state of rest. For $\Delta(t) \neq 0$ and $\overline{\Delta} \equiv 0$, the film vibrates. For $\overline{\Delta} \neq 0$, it rotates. These criteria enable derivation of the threshold characteristics of E_{ext} and E_{el} required for starting the vibration and the rotation of the liquid film.

To deepen our understanding of the physics underlying these criteria, we focus on the torques exerted on a disk of the liquid film. We recall that M_{am} and M_f , respectively, denote the maximum of the accelerating torque and the maximum static drag torque. We employ the symbol $\overline{M_a}$ for representing the time-averaged value of accelerating torque. $M_{\text{am}} < M_f$ implies that the accelerating torque cannot break the plastic structure of the liquid film, i.e., $\Delta(t) \equiv 0$, and the film remains static. For $M_{\text{am}} > M_f > \overline{M_a}$, the accelerating torque can intermittently break the plastic structure of the liquid film, i.e., $\Delta(t) \neq 0$, $\overline{\Delta} \equiv 0$, and the film vibrates. For $\overline{M_a} > M_f$, the accelerating torque can continuously drive the liquid film to rotate, i.e., $\overline{\Delta} \neq 0$, and the film rotates.

It should be pointed out that Eqs. (12)–(18) do not hold for ac fields with high frequencies. A frequency range exists for which the transient oscillates rapidly, causing the equivalent dipole moment per unit volume to depend on the frequency. This dependency affects $\Delta(t)$. It is therefore feasible that the ac motor will stop working when the frequency of E_{ext} is increased beyond some value. This conjecture has still to be experimentally verified. To estimate the frequency range, we note that in a static E_{ext} field, the polarization approach saturation occurs in about a picosecond [37]. For alternating E_{ext} , with frequencies up to about 10^{11} rad/s, it indeed was found that the polarization still periodically reaches the plateau level of a conventional transient triggered by a static E_{ext} when that field reverses its direction [38]. Accordingly, we expect Eqs. (12)–(18) to be valid for E_{ext} with frequencies below the far infrared microwave region. The experimentalists applied fields with frequencies up to 10^4 Hz. In regard to the foregoing, the equations derived in this section should be applicable for analyzing the experimentally observed features of the ac motor.

III. RESULTS AND DISCUSSION

In this section, we derive a series of specific characteristics of the ac motor and compare these to the experimentally observed phenomena. The experimental data, published in the literature, mainly specify the thresholds for the onset of rotation and their dependence on the frequencies and phase differences of E_{ext} and E_{el} . Accordingly, in Secs. III A and III B, respectively, we analyze the effects of these frequencies and phase differences on the EHD motions in the liquid film. For the analysis, we define the alternating external electric field and electrolysis voltage, respectively, as

$$E_{\text{ext}}(t) = E_0 \sin \omega_1 t \quad (19)$$

and

$$U_{\text{el}}(t) = E_{\text{el}}(t)l = U_0 \sin(\omega_2 t + \varphi), \quad (20)$$

where E_0 and U_0 , respectively, denote the amplitudes of the electric field and the voltage, $\omega_1 = 2\pi f_1$ and $\omega_2 = 2\pi f_2$ represent their angular frequencies, and φ is the initial phase of the electrolysis voltage. A change in the sign of E_{ext} or U_{el} corresponds to a reversal of the direction of these fields.

A. Relation between the characteristics of the EHD motions and the frequencies of the fields

To analyze the effect of ω_1 and ω_2 on the EHD motions, we start with focusing on the functional dependence of the driving source $\Delta(t)$ on these frequencies. For $\omega_1 \neq \omega_2$ and $\omega_1 < \omega_2$, upon inserting Eqs. (19) and (20) into Eq. (3), we obtain

$$\Delta(t) = \begin{cases} 0 & (|B(t)| < 2\tau_0) \\ [|B(t)| - 2\tau_0] \text{sign}[B(t)] & (|B(t)| \geq 2\tau_0), \end{cases} \quad (21)$$

where $\text{sign}[x]$ denotes a sign function,

$$B(t) = 2b \sin \omega_1 t \sin(\omega_2 t + \varphi), \quad (22)$$

and

$$b = \frac{\varepsilon_0(1 - 1/\varepsilon_r)E_0 U_0 \sin \theta_{\text{EJ}}}{2l}. \quad (23)$$

Equations (21) and (22) display that both the direction and the magnitude of the driving source $\Delta(t)$ vary with time. Moreover, these equations show that for $\Delta(t)$ to be a periodic function requires that the ratio of ω_1 to ω_2 be a rational number.

Just as for the dc motor, in correspondence with the experimental conditions, we set $\varepsilon_0 = 8.85 \times 10^{-12} \text{ C}^2 \cdot \text{N}^{-1} \cdot \text{m}^{-2}$, $\varepsilon_r = 80$, $E_0 U_0 \sin \theta_{\text{EJ}} = 7.2 \times 10^6 \text{ V}^2 \cdot \text{m}^{-1}$, $l = 2R = 3.1 \times 10^{-2} \text{ m}$, and $\mu = 10^{-3} \text{ Pa} \cdot \text{s}$ [15]. Also, for τ_0 , we used the same value as that employed for the dc motor, i.e., $\tau_0 = 6.77 \times 10^{-5} \text{ Pa}$ [15]. It was obtained by fitting the threshold fields of the dc motor, as expressed in Eq. (11), to the experimental results [15].

For $\varphi = 0$, using the parameters from the last paragraph and Eqs. (21)–(23), we compute and subsequently plot $\Delta(t)$ versus time t for different frequencies; see Fig. 1. This figure in combination with Eq. (21) indicate that $\bar{\Delta} \equiv 0$. According to the criteria derived in Sec. II B2, if $b > \tau_0$, then $\bar{\Delta} \equiv 0$ means that the film vibrates. On inserting Eq. (23) into the inequality $b > \tau_0$, the foregoing can be summarized as follows: for $\omega_1 \neq \omega_2$, $\omega_1 < \omega_2$, and $\varphi = 0$, when the applied fields satisfy

$$E_0 U_0 \sin \theta_{\text{EJ}} \geq \frac{2\tau_0 l}{\varepsilon_0(1 - 1/\varepsilon_r)}, \quad (24)$$

the liquid film will vibrate. Otherwise, it will be still. Currently, no experimental information exists on the thresholds for the onset of vibration. Accordingly, the above-derived expression for the threshold fields, i.e., Eq. (24), still requires experimental verification. However, our theoretical result that the film exhibits vibrations in ac fields with different frequencies is in full agreement with the experimental data, i.e., experimentally observed characteristic (b) of the ac motor cited in Sec. I above.

For $\varphi \neq 0$, the threshold field of the film's vibration depends on φ . So far, we did not succeed in deriving an analytical expression for this dependence. After experimental verification of Eq. (24), our above results indicate that future numerical analysis of the detailed effects of $\varphi \neq 0$ on the ac motor's vibration is warranted. It promises to provide important additional insights into the structure and interactions within the liquid film.

To analyze the dynamical characteristic of the film's vibration and its dependence on ω_1 and ω_2 , we compute $u(r, t)$ by numerically solving Eqs. (6), (22), and (23). We focus on the asymptotic case $b \gg \tau_0$, for which $2\tau_0$ is small

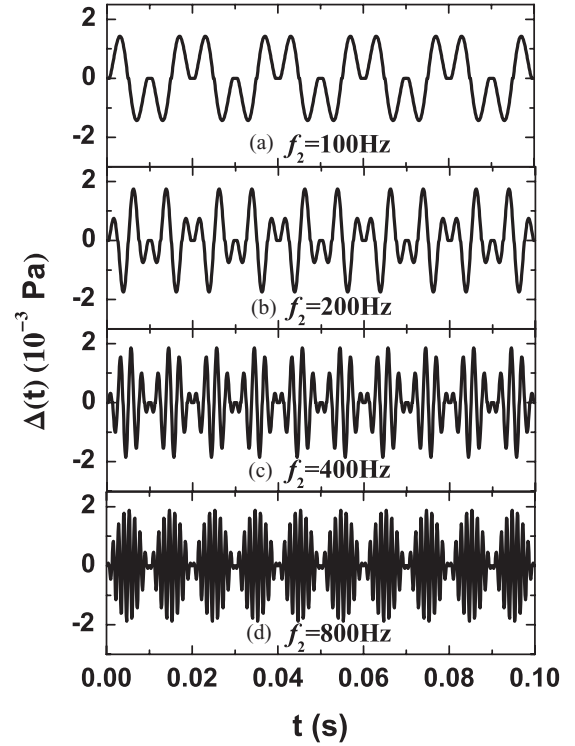


FIG. 1. $\Delta(t)$ vs time t for different values of frequency of the alternating voltage U_{el} : (a) $f_2 = 100 \text{ Hz}$, (b) $f_2 = 200 \text{ Hz}$, (c) $f_2 = 400 \text{ Hz}$, and (d) $f_2 = 800 \text{ Hz}$. The frequency of the alternating external electric field E_{ext} is $f_1 = 50 \text{ Hz}$.

enough to be ignored. This approximation enables one to express the driving source by Eq. (22). By substituting Eq. (21) together with Eq. (22) in Eq. (8), and using Eq. (6), after some rearrangements, we arrive at

$$u_V(r, t) = b \sum_{n=1}^{\infty} C_n J_1 \left(\frac{\kappa_n r}{R} \right) \{ \cos \gamma_{+,n} [-\cos(\omega_+ t + \varphi - \gamma_{+,n}) + e^{-a_n t} \cos(\varphi - \gamma_{+,n})] + \cos \gamma_{-,n} [\cos(\omega_- t + \varphi + \gamma_{-,n}) - e^{-a_n t} \cos(\varphi - \gamma_{-,n})] \}, \quad (25)$$

where $\omega_{\pm} = \omega_2 \pm \omega_1$ and $\gamma_{\pm,n} = \arctan(\omega_{\pm}/a_n)$.

The vibration of a point mass usually is described as a displacement. Similarly, the film's vibration can be expressed as the time integral of $u_V(r, t)$, namely,

$$l_V = b \sum_{n=1}^{\infty} C_n J_1 \left(\frac{\kappa_n r}{R} \right) \left[\frac{\cos \gamma_{-,n}}{\omega_-} \sin(\omega_- t - \gamma_{-,n}) - \frac{\cos \gamma_{+,n}}{\omega_+} \sin(\omega_+ t - \gamma_{+,n}) \right], \quad (26)$$

where l_V presents the torsion displacement of a liquid film disk with radii r and $r + dr$ as a function of time; $\varphi = 0$ and the transient-state terms are omitted. By inserting in Eq. (26) the same parameter values used to produce Fig. 1, we calculate the torsion displacement as a function of time and radii. The results are plotted in Fig. 2. By comparing Figs. 1 and 2, we find that the shapes of the film's vibration and the corresponding driving source are similar, which is characteristic of a forced vibration. Equation (26) and Fig. 2 show the following:

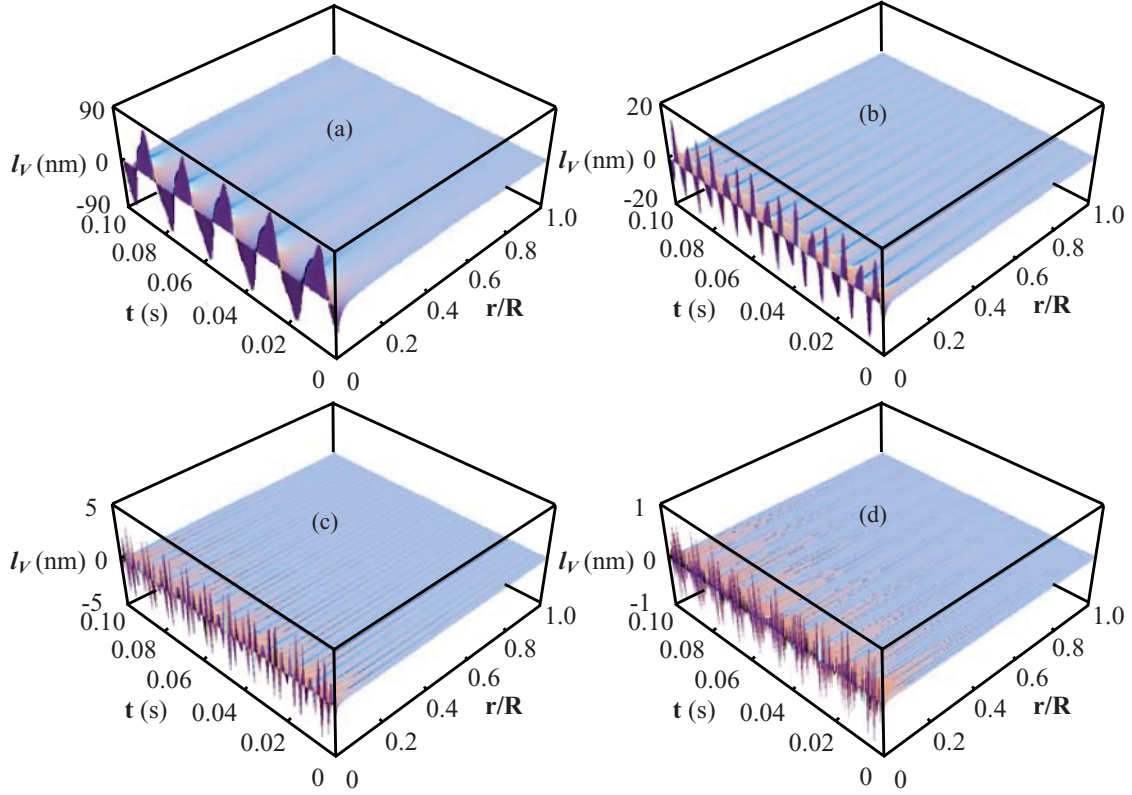


FIG. 2. (Color online) Torsion displacement l_V as a function of time t and r/R (the radius r in units of R). The parameters employed for describing the film are the same as those used to produce Fig. 1. The frequencies of the fields for (a)–(d), respectively, correspond with those of Figs. 1(a)–1(d).

(i) The amplitude of the vibration is maximal near the center of the film. It is zero at the center, as easily learned by inserting $r = 0$ into Eq. (26), resulting in $J_1(0) = 0$ causing $l_V = 0$.

(ii) The amplitude of the vibration decreases strongly as the radius increases.

(iii) When f_2 approaches f_1 , the liquid film's vibration characteristics start to resemble those of a simple harmonic motion.

(iv) On increasing f_2 , the amplitude of the vibration decreases.

(v) For sufficiently large values of f_2 , beating occurs. An example is presented in Fig. 2(d). Its vibration frequency is twice as much as the value of f_1 .

Currently, the reported experimental data is insufficient for verification of our theoretical findings (i)–(iv). As to our theoretical finding (v), it is in agreement with the experimental phenomenon of a beat vibration; see characteristic (b) of the ac motor cited in Sec. I. However, the experimentalists did not detail the beating characteristics [10–12]. Experimental verification of findings (i)–(iv) is highly desirable. These findings contain a wealth of physical information. Though the computed torsion displacements of the ring liquid films are very small ($\sim 10^{-9}$ – 10^{-8} m; see Fig. 2), the future computation of superpositions of vibration waves spreading across the film should enable quantitative comparisons with experiments.

B. Relation between the characteristics of the EHD motions and the phase differences of the fields

For $\omega_1 = \omega_2 = \omega$ ($f_1 = f_2 = f$), φ represents the phase difference between the crossed E_{cl} and E_{ext} fields. To analyze the impact of φ on the EHD motions of the liquid film, we derive the functional dependence of the driving force $\Delta(t)$ on φ . The insertion of Eqs. (19), (20), and (23) into Eq. (3) shows that $\Delta(t)$ is the sum of the following two terms: $B_c = b \cos \varphi - 2\tau_0$ and $B_t = -b \cos(2\omega t + \varphi)$. Here the subscript c indicates that B_c is time independent, and the subscript t indicates that B_t is time dependent. On recalling that $\Delta(t)$ is a function of the torque, the physical meaning of these terms becomes apparent:

(i) $B_c \geq 0$ (analogous to $\Delta(t) \geq 0$, that is, $B(t) \geq 2\tau_0$ for the dc motor) indicates that the accelerating torque continuously breaks up the field-induced plasticity of the liquid film, and the expression for the driving source is $\Delta(t) = B_c + B_t$. As discussed in Sec. II B2 and the following, from Eqs. (18) and (29), one finds that the film will rotate under the circumstances because $\bar{\Delta} = B_c$.

(ii) $B_c < 0$ means that the constant component of the accelerating torque can only partly destroy the plastic microstructure of the liquid film. The onset of any motion in the film requires that the time-dependent component of the accelerating torque overcomes the resistance from the apparent yield stress, $\tau_a = \tau_0 - (b \cos \varphi)/2$. Whenever this time-dependent component cannot overcome the resistance

arising from τ_a , $\Delta(t) \equiv 0$, and the film remains static. Otherwise, the expression for $\Delta(t)$ is similar to the one detailed in the second line of Eq. (21). As discussed below, the film exhibits vibrational movements under the circumstances.

Statements (i) and (ii) can be summarized as follows:

$$\Delta(t) = \begin{cases} 0 & (B_c < 0 \text{ and } |B_t| < 2\tau_a) \\ (|B_t| - 2\tau_a) \text{sign}[B_t] & (B_c < 0 \text{ and } |B_t| \geq 2\tau_a) \\ B_c + B_t & (B_c \geq 0). \end{cases} \quad (27)$$

To obtain the threshold fields for starting the vibration and the rotation of the liquid film motor, recalling the criteria presented in Sec. II B 2, we have calculated the maximum value and the time-averaged value of $\Delta(t)$, that is,

$$\Delta_{\max} = \begin{cases} 0 & (B_c < -b) \\ b(1 + \cos \varphi) - 2\tau_0 & (B_c \geq -b), \end{cases} \quad (28)$$

and

$$\bar{\Delta} = \begin{cases} 0 & (B_c < 0) \\ b \cos \varphi - 2\tau_0 & (B_c \geq 0). \end{cases} \quad (29)$$

On equalizing the second expressions in Eqs. (28) and (29), respectively, to zero, one obtains, from Eq. (27),

$$E_0 U_0 \sin \theta_{\text{EJ}} = \frac{4\tau_0 l}{\varepsilon_0(1 - 1/\varepsilon_r)(1 + \cos \varphi)}, \quad (30)$$

and

$$E_0 U_0 \sin \theta_{\text{EJ}} = \frac{4\tau_0 l}{\varepsilon_0(1 - 1/\varepsilon_r) \cos \varphi}. \quad (31)$$

According to the criteria derived in Sec. II B 2, Eqs. (30) and (31), respectively, determine the threshold fields for the onset of vibration and rotation of the ac motor.

By inserting in Eqs. (30) and (31) the same parameter values used to produce Figs. 1 and 2, we calculate and subsequently plot in Fig. 3 the values of the threshold fields as a function of φ . Figure 3 illustrates that the critical lines $\Delta_{\max} = 0$ and $\bar{\Delta} = 0$, respectively, matching Eqs. (30) and (31), divide the graph into three sections. These sections correspond to three states of motion of the film: state of rest, vibration, and rotation. Figure 3 illustrates that on fixing φ and increasing $E_0 U_0 \sin \theta_{\text{EJ}}$ from zero, the film sequentially passes from a state of rest [$\Delta(t) \equiv 0$] to vibration ($\Delta_{\max} > 0$ and $\bar{\Delta} = 0$), and then to rotation ($\bar{\Delta} \neq 0$). On fixing $E_0 U_0 \sin \theta_{\text{EJ}}$ and increasing φ , only one crossover appears and the film either changes from rotation to vibration, or from vibration to a state of rest.

Figure 3 shows that $\bar{\Delta} = 0$, i.e., our computed black solid line, is in excellent agreement with the experimental data. As such, it shows that our model explains also the experimental observed characteristic (a) of the ac motor cited in Sec. I. In an attempt to explain these data, the experimentalists assumed that at the threshold points for the onset of rotation, the time average of $E_{\text{ext}} U_{\text{el}}$, i.e., $\bar{E}_{\text{ext}} U_{\text{el}}$, should be constant [11]. Our theoretical analysis of the EHD motions presented above, in particular Eq. (31), provides the theoretical foundation for this assumption. As to our predicted $\Delta_{\max} = 0$ (red dashed line), it has yet to be experimentally verified.

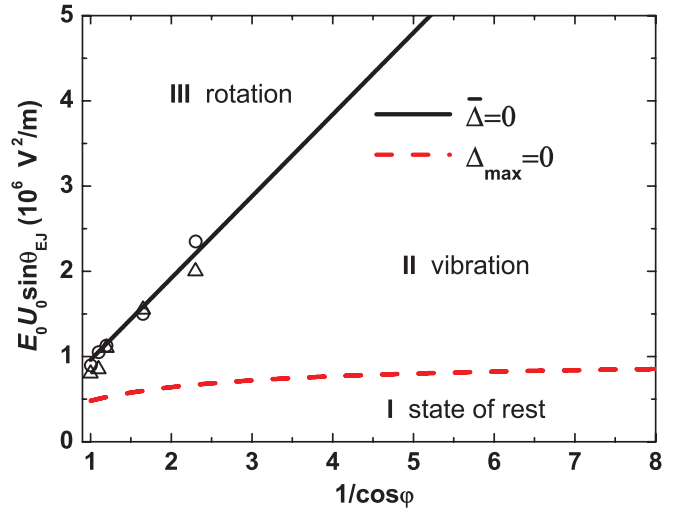


FIG. 3. (Color online) Values of the threshold fields as a function of φ . The dashed and solid lines, respectively, represent the computed $\Delta_{\max} = 0$ and $\bar{\Delta} = 0$. Circles and triangles represent experimental data extracted from Fig. 4 of Ref. [11]. The circles were obtained for $E_0 = 50$ kV/m and the triangles for $E_0 = 100$ kV/m.

Figure 3 indicates that the larger the phase difference, the larger are the threshold amplitudes of the electric fields required for the onset of vibration or rotation of the film. The underlying physical reason is easily understood on recalling that $B(t) = b \cos \varphi - b \cos(2\omega t + \varphi)$ represents the accelerating torque exerted on the liquid film. An increase in the phase difference will weaken the ability of the accelerating torque to destroy the plastic structure of the liquid film because the maximal and the time average of the accelerating torque decreases as φ increases.

On comparing the order of magnitudes of the threshold fields of the ac and dc motors, i.e., on equating Eqs. (31) and (11) and inserting the same parameters used to produce Fig. 1, one obtains

$$(E_0 U_0 \sin \theta_{\text{EJ}} \cos \varphi)_{\text{AC}} = 2(E_{\text{ext}} U_{\text{cur}} \sin \theta_{\text{EJ}})_{\text{DC}} \sim 10^6 \text{ V}^2/\text{m}. \quad (32)$$

Here subscripts AC and DC, respectively, denote the physical quantities of ac fields and dc fields. This result fully agrees with the experimental data; see Figs. 2 and 4 in Ref. [11]. The agreement accentuates the self-consistency of our model. The consistency mainly stems from the central role played by the Bingham plastic fluid's yield stress. It emphasizes that the polar superdomain CD chains are the main players determining the interactions, structure, and dynamics of the polar liquid film. This role indeed is corroborated by the experimental data [11,12] and our theoretical findings presented in our previous paper [15], which revealed that the magnitudes of the threshold fields are of the same order for liquids with different electrical conductivity, viscosity, dielectric constant, and density [11,12,15]. This conclusion indeed also is backed up by very recent experiments employing very different measuring techniques, which revealed that dissimilar polar liquids (e.g., water, methanol, ethanol, iso-propanol, and acetic acid), polarized by their substrate, have very similar near-surface-zones structures [39].

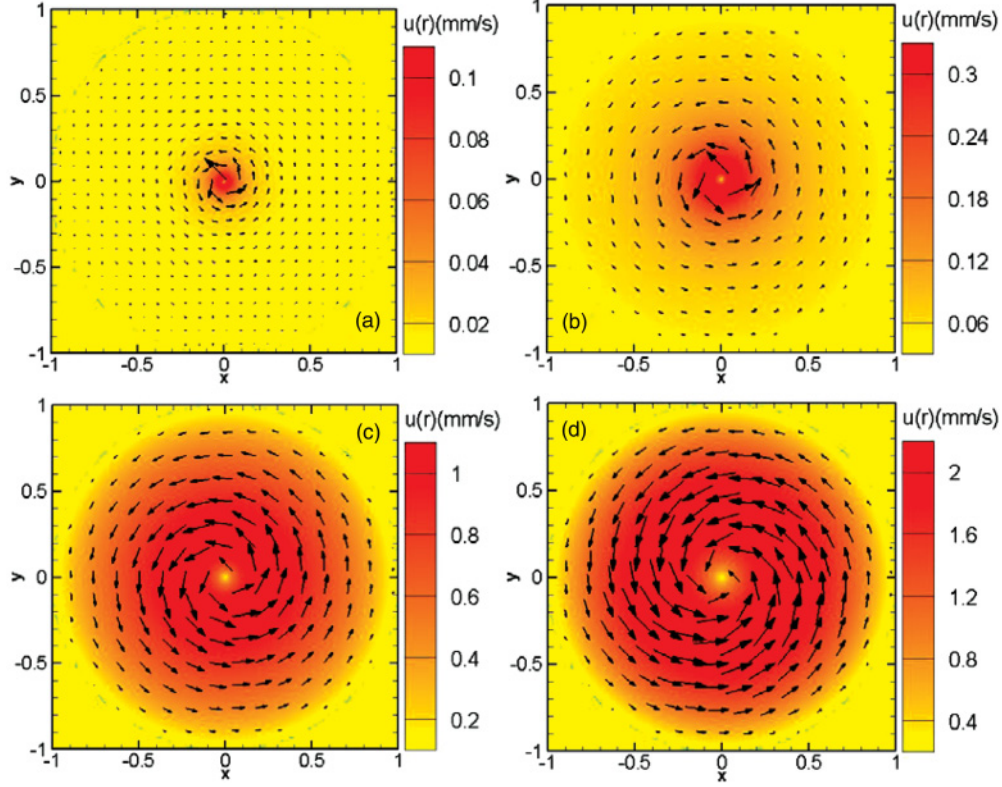


FIG. 4. (Color online) 2D velocity fields of the square liquid film at different times: (a) $t = 0.1$ s, (b) $t = 1$ s, (c) $t = 10$ s, and (d) $t = 100$ s. x and y coordinates are in units of R . For $t \geq 100$ s, the velocity fields do not change.

As to the characteristics of the EHD motions and their dependence on φ , the features of the vibrations are similar to those of Fig. 2 discussed in Sec. III A. The underlying reason for the similarity is that for $B_c < 0$, the driving source $\Delta(t)$ is described by the first two lines of Eq. (27), which may be obtained from Eq. (21) by replacing $B(t)$ with B_t , and τ_0 with τ_a . Accordingly, for $-b < B_c < 0$, the film vibrates. As to the features of the vibration, we noted in Sec. III A that the film exhibits forced vibrations, and for $\omega_1 = \omega_2 = \omega$, the vibration is that of a simple harmonic vibration with a frequency equal to that of the driving source $\Delta(t)$, i.e., $2f$. Moreover, it should be noted that on fixing b and increasing φ , the amplitude of the vibration decreases because $\Delta(t)$ decreases with increasing φ .

To analyze the characteristics of the rotation of the liquid film, we derive the expression for $u(r, t)$. Using Eqs. (13) and (15), and the third expression in Eq. (27), we have

$$u(r, t) = u_{DC}^{B_c}(r, t) + u_V^{B_i}(r, t), \quad (33)$$

where $u_{DC}^{B_c}(r, t)$ equals $u_{DC}(r, t)$ defined in Eq. (9), with the minor alteration that B_c substitutes for $\Delta(t)$. As to $u_V^{B_i}(r, t)$, it is expressed by Eq. (25) when $\gamma_{2,n} = \arctan(2\omega/a_n)$ substitutes for $\gamma_{+,n}$ and $\pi/2$ substitutes for $\gamma_{-,n}$. Equation (33) indicates that for the ac motor, rotation of the film comprises not only rotation modes but also vibration modes. No such situation arises in the dc motor. However, as our calculations reported in the next paragraph show, the rotation of the liquid film in ac fields, for $\omega_1 = \omega_2$, exhibits similar evolution characteristics to those in dc fields. The underlying reason is that the

contributions of vibration modes to the linear velocity are significantly smaller than those of rotation modes.

Employing Eq. (33) and the same parameters used to produce Fig. 1, we compute for $\varphi = 0$ the 2D velocity fields of the square liquid film at different times. In Fig. 4, we plot these 2D velocity fields. This figure illustrates that the points near the center of the film start to rotate earlier than those farther away from it. As time elapses, the location of the maximum of the linear velocity moves away from the center of the film. For the steady state rotation, i.e., Fig. 4(d), it holds that the linear velocity has its maximum around R/e .

Our computed Fig. 4 is in qualitative agreement with the snapshots of the experimental movies [35]. According to the movies, immediately after application of the electric fields, the rotating spiral lines emerging near the center of the films indicate that points close to this center rotate earlier and faster than those farther away from it. Movie 8 [35] shows that with the passage of time, the spiral-like rotation lines first spread all over the film and subsequently disappear. In the steady state, only circled rotation lines cover the film.

Using the same parameters as in Fig. 4 and Eq. (33), we compute and subsequently plot in Fig. 5 the profiles of the linear velocity for different φ at time $t = 100$ s. Figure 5 illuminates that in the steady state, the linear velocity decreases gradually as φ increases. This result can be understood by examining Eq. (33), $B_c = b \cos \varphi - 2\tau_0$, and Fig. 3. On fixing b , B_c (i.e., Δ) decreases with increasing φ . The underlying physical causes are the same as those presented above for explaining Fig. 3, i.e., an increase in the phase difference will weaken the ability of the accelerating torque to destroy the

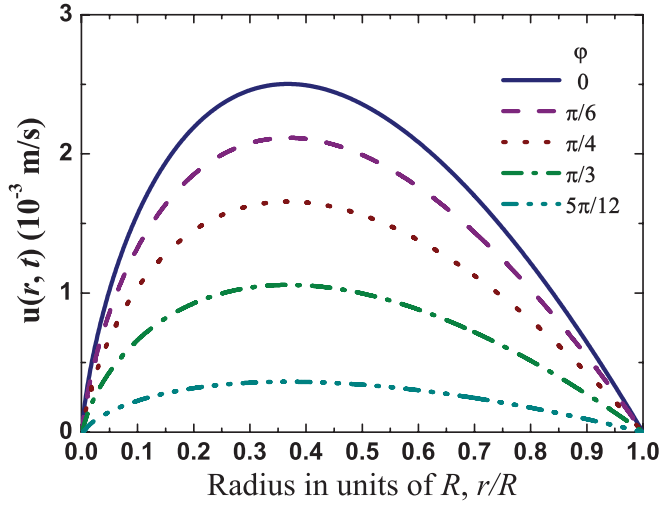


FIG. 5. (Color online) The profiles of the linear velocity for various values of φ at time $t = 100$ s.

plastic structure of the liquid film because the maximal and the time average of the accelerating torque decreases as φ increases.

For a special case, $\varphi = \pi/2$, the liquid film can only vibrate. In other words, even for fields much higher than those employed to compute Figs. 4 and 5, the film cannot rotate because for $\varphi = \pi/2$, $B_c < 0$ and $\bar{\Delta} \equiv 0$ according to Eq. (29). For the asymptotic case $b \gg \tau_0$, this vibration is determined by Eq. (25) when $\gamma_{2,n} = \arctan(2\omega/a_n)$ is substituted for $\gamma_{+,n}$, and $\pi/2$ is substituted for $\gamma_{-,n}$.

Currently, no experimental data is available to verify our theoretical results discussed in the last two paragraphs. Their experimental study could provide additional insight into the dynamics in the liquid film motors.

IV. SUMMARY

In this paper, we investigated EHD motions in polar liquid film motors driven by ac electric fields. In our theoretical analyses, we focus on the driving source $\Delta(t)$. It encodes the competition between the accelerating torque and the plasticity of the film, both of which are induced by the applied ac fields. Our main finding is that by analyzing $\Delta(t)$, it is possible to analytically derive dynamical characteristics of the film, such as

- (a) threshold conditions for the onset of its vibration or rotation,
- (b) impact of the frequencies of the ac fields and their phase differences on its EHD motions, and
- (c) its velocity fields.

We show that our model accounts for all of the major significant experimentally observed characteristics of the EHD motions of the ac motor. (The experimental measurements were carried out by a different research group.) For the limited available quantitative experimental data, we obtained a quantitative agreement between our computed values and the measured ones. For the abundant qualitative experimental findings, our analyses showed qualitative agreement between our computations and the experimental observations. In a previous paper, we already showed this to be true for the

dc motor [15]. Our model's main predictions, derived in this paper and in full agreement with the experimental ones, are as follows: (1) Rotation of the film requires that the frequencies of E_{ext} and E_{el} are exactly the same and their magnitudes surpass a threshold, which is determined by Eq. (31). (2) ac fields with different frequencies cannot induce rotation but produce vibrational movements. (3) The EHD motions strongly depend on the polarization induced by E_{ext} . However, these motions are little affected by the liquid's electrical conductivity, viscosity, dielectric constant, and density.

Our model also predicts a series of features of liquid film motors, which are of potential technological importance, but were not yet experimentally observed. Two main predicted features among them are as follows: (4) Vibrations may also be induced by fields with the same frequencies. (5) The threshold for the onset of vibrations is a function of the amplitudes, frequencies, and phase difference of the ac fields, as well as characteristics of the film. Future research directed at their experimental verification is warranted. It is our conjecture that no new techniques have to be developed for their experimental confirmation; the methods hitherto employed by the experimentalists to study the ac and dc motors suffice [11]. We expect such research also to provide important additional support for our model or to enable improving it.

In Table I of the Supplemental Material [40], we summarize the characteristics of the dynamics of the ac liquid film motor theoretically derived in this paper. For comparison, we also note the characteristics of the dc liquid film motor, which we theoretically obtained in our previous study [15]. For both type of motors, we note the agreement between our theoretical results and the experimental data.

V. CONCLUSIONS

The discussions of Sec. III, the results summarized in Sec. IV, and Table I in the Supplemental Material [40] lead us to several conclusions.

(i) In our computations, required to compare our theoretical findings to the experimentally measured ones, we employed one fitted parameter, i.e., the yield stress τ_0 of the water film. As noted in Sec. III A, we set τ_0 to a value ensuring that for the dc motor, the threshold fields as expressed by Eq. (11) reproduce the experimentally observed ones. In a previous publication [15], we showed that upon employing this value, all of our theoretically derived characteristics of the EHD motions of the dc motor fully conform to the measured ones (see Table I in the Supplemental Material [40]). In this paper, we showed that also in the case of the ac motor, this value of τ_0 leads to full agreement between its computed features and experimentally observed ones (See prediction (1) in Sec. IV and Table I in the Supplemental Material [40]). Our successful modeling of both motor types indicates that τ_0 adequately represents the film's yield stress. Moreover, it exposes our model's internal consistency.

(ii) Our model of the polar liquid film motor is a phenomenological one. We expect that development of a quantitative model, based on first principles, will shed more light on the various aspects of the motor and optimize its technological applications. Such a model mainly should include a detailed QFT description of the liquid film's CDs,

their organization, and their dynamics induced by applied electric fields. In our preliminary attempts to develop such a model, we noted that our current and previous paper's findings suggest several promising research projects, which we anticipate to lead to the development of a quantitative model for the liquid film motor. In paragraphs (iii) and (iv) below, we will elaborate on some facets of these projects.

(iii) In our previous paper [15], we investigated characteristics of τ_0 . Our main findings were as follows: τ_0 is independent of the electrical conductivity, viscosity, and density of the liquid; τ_0 is only slightly affected by the liquid's relative dielectric constant ϵ_r ; the magnitudes of τ_0 for widely different polar liquids (e.g., water, aniline, anisole, chlorobenzene, diethyleoxalate) are of the same order; τ_0 depends on the thickness of the liquid film; and τ_0 is a strongly decreasing function of the fraction of glycerin included in the liquid. These characteristics indicate that τ_0 mainly depends on the properties of the CDs and the supercoherence among them, with glycerin seemingly reducing the coherence.

In our previous paper on the dc motor [15], we deduced that the strong dependence of τ_0 on the coherence of the film's molecules provides additional justification for one of the central assumptions of our model, i.e., the CDs constitute a significant component of polar liquid film motors. This paper's finding, i.e., in which for the ac motor also the characteristics of our computed EHD motions agree with the experimental observed ones, provides additional justification for this assumption. Our theoretical results thus corroborate the conjecture, proposed by the experimentalists, that the intrinsic polarity of the liquid's molecules is the crucial quality of the film enabling the creation of the polar liquid film motor. Within this context, we recall that experiments showed that films

composed of polar liquids wherein no hydrogen bonds exist can be used to produce a liquid film motor. However, applying electric fields to films composed of molecules which do not have a significant asymmetric electric charge distribution, e.g., 1-dodecene, do not lead to any rotation [11]. The foregoing suggests that future research projects, directed at studying the dependence of τ_0 on the features of the coherent oscillations of polar liquid molecules, might enable the derivation of the value of τ_0 from first principles.

(iv) The substrate of the film very likely also affects the CDs and their organization. However, to the best of our knowledge, hitherto, neither experimental nor theoretical studies of the effects of the substrate on τ_0 have been undertaken. Until now, in the liquid film motors, the films have been placed on ordinary blank printed circuit boards. We expect future research projects, focusing on the identification of specific relations between the characteristics of the substrate and the EHD motions of the film, to shed additional light on the underlying forces affecting the dynamics in liquid film motors.

We conclude with noting that we expect that all research directions, noted in Secs. II–V, ultimately will lead to the delineation of those film characteristics required for optimizing the motors.

ACKNOWLEDGMENTS

Our work has been supported in part by the National Basic Research Program of China (Grant No. 2007CB815105) and the National Natural Science Foundation of China (Grant No. 11074300). Z.Q.L. and S.R.J. gratefully thank Dr. Tamar A. Yinnon for her patient guidance, encouragement, enlightening discussions, warm support, and reading of this manuscript.

-
- [1] R. A. L. Jones, *Soft Condensed Matter* (Oxford University Press, New York, 2002).
 - [2] P. Nelson, *Biological Physics: Energy, Information, Life* (Freeman, New York, 2003).
 - [3] T. M. Squires and S. R. Quake, *Rev. Mod. Phys.* **77**, 977 (2005).
 - [4] H.-C. Chang and L. Y. Yeo, *Electrokinetically-driven Microfluidics and Nanofluidics* (Cambridge University Press, New York, 2010).
 - [5] A. A. Sonin, *Freely Suspended Liquid Crystalline Films* (Wiley, New York, 1998).
 - [6] S. Faetti, L. Fronzoni, and P. A. Rolla, *J. Chem. Phys.* **79**, 5054 (1983).
 - [7] S. W. Morris, J. R. de Bruyn, and A. D. May, *Phys. Rev. Lett.* **65**, 2378 (1990).
 - [8] Z. A. Daya, S. W. Morris, and J. R. de Bruyn, *Phys. Rev. E* **55**, 2682 (1997).
 - [9] A. Ramos, H. Morgan, N. G. Green, and A. Castellanos, *J. Phys. D* **31**, 2338 (1998).
 - [10] R. Shirsavar, A. Amjadi, N. H. Radja, M. D. Nirry, M. R. R. Tabar, and M. R. Ejtehadi, e-print [arXiv:condmat/0605029](https://arxiv.org/abs/condmat/0605029).
 - [11] A. Amjadi, R. Shirsavar, N. H. Radja, and M. R. Ejtehadi, *Microfluid Nanofluid* **6**, 711 (2009).
 - [12] R. Shirsavar, A. Amjadi, A. Tonddast-Navaei, and M. R. Ejtehadi, *Exp. Fluids* **50**, 419 (2011).
 - [13] E. V. Shiryayeva, V. A. Vladimirov, and M. Y. Zhukov, *Phys. Rev. E* **80**, 041603 (2009).
 - [14] F. P. Grosu and M. K. Bologa, *Surf. Eng. Appl. Electrochem.* **46**, 43 (2010).
 - [15] Z. Q. Liu, Y. J. Li, G. C. Zhang, and S. R. Jiang, *Phys. Rev. E* **83**, 026303 (2011).
 - [16] E. Del Giudice, E. C. Fuchs, and G. Vitiello, *Water (Seattle)* **2**, 69 (2010).
 - [17] E. Del Giudice, P. R. Spinetti, and A. Tedeschi, *Water* **2**, 566 (2010).
 - [18] M. V. Gandhi and B. S. Thompson, *Smart Materials and Structures* (Chapman & Hall, London, 1992).
 - [19] E. Del Giudice, G. Preparata, and G. Vitiello, *Phys. Rev. Lett.* **61**, 1085 (1988).
 - [20] S. Sivasubramanian, A. Widom, and Y. N. Srivastava, *Physica A* **345**, 356 (2005); E. Del Giudice and G. Vitiello, *Phys. Rev. A* **74**, 022105 (2006).
 - [21] G. Preparata, *QED Coherence in Matter* (World Scientific, Singapore, 1995); *Phys. Rev. A* **38**, 233 (1988); R. Arani, I. Bono, E. Del Giudice, and G. Preparata, *Int. J. Mod. Phys. B* **9**, 1813 (1995); E. Del Giudice and G. Preparata, in *Macroscopic*

- Quantum Coherence*, edited by E. Sassaroli, Y. N. Srivastava, J. Swain, and A. Widom (World Scientific, Singapore 1998); E. Del Giudice, *J. Phys. Conf. Ser.* **67**, 012006 (2007); M. Buzzacchi, E. Del Giudice, and G. Preparata, *Int. J. Mod. Phys. B* **16**, 3771 (2002); E. Del Giudice, A. Galimberti, L. Gamberale, and G. Preparata, *Mod. Phys. Lett. B* **9**, 953 (1995); E. Del Giudice, M. Fleischmann, G. Preparata, and G. Talpo, *Bioelectromagnetics* **23**, 522 (2002); E. Del Giudice, G. Preparata, and M. Fleischmann, *J. Elec. Chem.* **482**, 110 (2000).
- [22] S. Sivasubramanian, A. Widom, and Y. N. Srivastava, *Physica A* **301**, 241 (2001); *Int. J. Mod. Phys. B* **15**, 537 (2001); *Mod. Phys. Lett. B* **16**, 1201 (2002); *J. Phys. Condens. Matter* **15**, 1109 (2003); C. Emary and T. Brandes, *Phys. Rev. E* **67**, 066203 (2003); M. Apostol, *Phys. Lett. A* **373**, 379 (2009).
- [23] C. A. Yinnon and T. A. Yinnon, *Mod. Phys. Lett. B* **23**, 1959 (2009).
- [24] C. Huang *et al.*, *Proc. Natl. Acad. Sci. USA* **106**, 15214 (2009).
- [25] J. M. Zheng, W. C. Chin, E. Khijniak, E. Khijniak Jr., and G. H. Pollack, *Adv. Coll. Inter. Sci.* **127**, 19 (2006).
- [26] Jampa Maruthi Pradeep Kanth, S. Vemparala, and R. Anishetty, *Phys. Rev. E* **81**, 021201 (2010).
- [27] H. Jansson, R. Bergman, and J. Swenson, *Phys. Rev. Lett.* **104**, 017802 (2010).
- [28] L. Noirez, P. Baroni, and H. Mendil-Jakani, *Polym. Int.* **58**, 962 (2009).
- [29] E. E. Fenn, D. B. Wong, and M. D. Fayer, *Proc. Natl. Acad. Sci. USA* **106**, 15243 (2009).
- [30] H. Yoo, R. Paranj, and G. H. Pollack, *J. Phys. Chem. Lett.* **2**, 532 (2011).
- [31] A. Widom, J. Swain, J. Silverberg, S. Sivasubramanian, and Y. N. Srivastava, *Phys. Rev. E* **80**, 016301 (2009).
- [32] L. Luo, S. H. L. Klapp, and X. S. Chen, *J. Chem. Phys.* **135**, 134701 (2011); L. Luo and X. S. Chen, *Sci. China Phys. Mech. Astron.* **54**, 1555 (2011).
- [33] E. C. Fuchs, P. Baroni, B. Bitschnau, and L. Noirez, *J. Phys. D* **43**, 105502 (2010).
- [34] E. C. Bingham, An Investigation of the Laws of Plastic Flow, Bur. Stand. Bulletin (US) **13**, 309 (1916); J. F. Steffe, *Rheological Methods in Food Process Engineering* (Freeman, East Lansing, MI, 1996).
- [35] See <http://www.softmatter.cscm.ir/FilmMotor/> for experimental movies.
- [36] R. Courant and D. Hilbert, *Methods of Mathematical Physics*, Vol. 1 (Wiley, New York, 1989).
- [37] D. Bertolini, M. Cassetari, and G. Salvetti, *J. Chem. Phys.* **76**, 3285 (1982).
- [38] N. P. Adhikari, H. Paudyal, A. Tiwari, and M. Johri, *J. Mol. Liq.* **158**, 80 (2011).
- [39] B. Chai and G. H. Pollack, *J. Phys. Chem. B* **114**, 5371 (2010).
- [40] See Supplemental Material at <http://link.aps.org/supplemental/10.1103/PhysRevE.85.036314> for liquid film motors' theoretical characteristics, predicted by our model, and experimental observed ones.